Molecular Crystals and Liquid Crystals

Publication details, including instructions for authors and subscription information:
http://www.tandfonline.com/loi/gmcl16

Determination of Nematic Liquid Crystal Elastic and Dielectric Constants from Birefringence Experiments

Craig Maze [a] & Dave Johnson [b]

[a] Motorola, Inc., 5005E. McDowell Road, Phoenix, Arizona, 85008

[b] Department of Physics and Liquid Crystal Institute, Kent State University, Kent, Ohio, 44242

Version of record first published: 28 Mar 2007.

To cite this article: Craig Maze & Dave Johnson (1976): Determination of Nematic Liquid Crystal Elastic and Dielectric Constants from Birefringence Experiments, Molecular Crystals and Liquid Crystals, 33:3-4, 213-225

To link to this article: http://dx.doi.org/10.1080/15421407608084297

Mol. Cryst. Liq. Cryst., 1976, Vol. 33, 213–225
Printed in Holland

Determination of Nematic Liquid Crystal Elastic and Dielectric Constants from Birefringence Experiments†

CRAIG MAZE
Motorola, Inc., 5005E. McDowell Road, Phoenix, Arizona 85008

and

DAVE JOHNSON
Department of Physics and Liquid Crystal Institute, Kent State University, Kent, Ohio 44242

(*Received June 16, 1975; in final form October 20, 1975*)

A non-linear least squares technique was used to determine k_{11}, k_{33}, ε_1 and ε_2 by comparing data from a single birefringence vs. voltage experiment. Liquid crystal optical cells with parallel orientation were used to generate the birefringence-voltage curve from which the parameters were determined. Cell thickness was found to have a strong influence on parameter estimates which could not be accounted for in terms of the physical model used. In spite of the thickness dependence, the four parameters mentioned above could be estimated to a high degree of precision using techniques described herein.

INTRODUCTION

Accurate measurement of Frank elastic constants,[1] of liquid crystal mixtures and pure compounds is an important area related to display device design and to greater physical understanding of liquid crystals. This paper demonstrates how two of the three elastic constants, splay and bend, can be determined from optical birefringence measurements taken with an optical cell

---

† Research supported in part by the National Science Foundation under Grant DMR-74-13173.

having parallel orientation. Both components of the uniaxial dielectric tensor can also be determined from the same experimental data.

Previous theoretical work in this area was performed by Deuling.[2] In his paper a general theory was presented which should be valid for arbitrary dielectric anisotropy. He applied the theory to the experimental data of Gruler and Meier,[3] for a nematic of low anisotropy ($\varepsilon_1 - \varepsilon_2 = 0.034$). Critical voltage and a ratio of elastic constants were obtained from the experimental data using a non-linear curve fitting algorithm.[2] Agreement between theory and experiment was reported to have been good at low applied cell voltage, but deviate considerably at higher voltages. The discrepancy was not explained, but as will be shown there are two factors which influence the difference between theory and experiment, particularly at low voltage.

This paper is an extension of the earlier work to materials of high positive dielectric anisotropy ($\varepsilon_1 - \varepsilon_2 = 14.5$) and to cells of different thickness. The calculation procedure was modified and improved to provide confidence limits for parameter estimates based on Deuling's theory. Finally, the adjustable parameter set was changed and enlarged from $\{V_c$ and $\kappa\}$ appearing in Ref. 2, to $\{k_{11}, k_{33}, \varepsilon_1, \varepsilon_2, d\}$†.

The remainder of this paper will consist of a summary of the relevant portion of Deuling's work; a description of the experimental method and materials used; an outline of the calculation procedure; and the results, some of which are calculation dependent.

EXPERIMENTAL

The optical apparatus used to measure change in birefringence with applied electric field is shown schematically in Figure 1. Vertically polarized He–Ne laser light is incident upon a homogeneously oriented nematic liquid crystal with zero twist whose director (and hence optic axis) is at 45° to the vertical and in the plane of the film. Below the voltage threshold for optic axis distortion the intensity of transmitted light at the photodiode depends upon

1) incident light beam intensity
2) reflections
3) polarizer-analyser extinction ratio
4) light scattering and depolarization due to thermal fluctuations of the director

---

† Symbols explained in glossary.

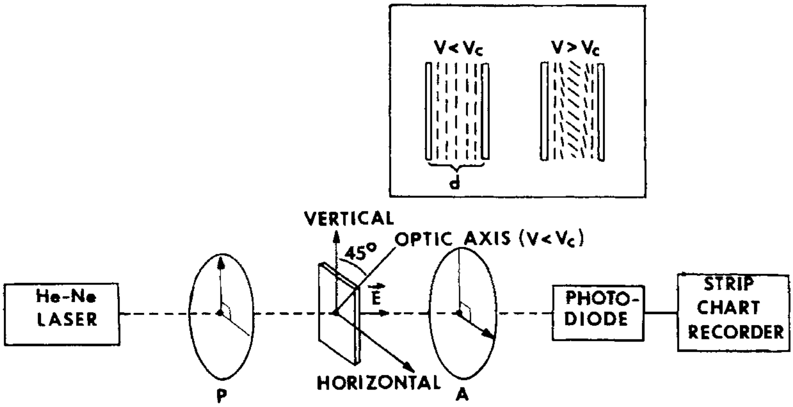

FIGURE 1 Schematic of optical system. The optic axis of the undistorted sample is 45° from the vertical and in the plane of the film. *INSET*: Schematic of molecular distribution below and above the critical voltage V_c.

5) the phase shift between the ordinary and extraordinary rays due to birefringence of the sample.

Of these only (4) and (5) are affected by the applied voltage, and (5) dominates the voltage dependence of the transmitted light. Neglecting the others, the transmitted intensity may be written as:

$$I = I_0 \sin^2(\pi\delta_c) \tag{1}$$

and

$$\delta_c = \frac{d}{\lambda}(n_e - n_0) \tag{2}$$

n_e and n_0 were measured in a separate experiment with an Abbe' refractometer using oriented samples and polarized light. They were found to be 1.6816 and 1.5054 respectively. The least count was ±0.005; the light-dark interface being not quite as abrupt as for normal isotropic liquids.

Above V_c Eq. (2) may be written[4]

$$\delta_c = \frac{1}{\lambda}\int_0^d (n(z) - n_0)\,\mathrm{d}z \tag{3}$$

where

$$n(z) = \frac{n_e n_0}{\sqrt{n_e^2 \sin^2 \phi + n_0^2 \cos^2 \phi}} \tag{4}$$

All measurements were made at 24 ± 1°C, which is far below the clearing point of the liquid crystal mixture used. The applied electric field is an amplitude ramped 1000 Hz square wave. It was found that a ramp rate of 1 millivolt per minute was sufficiently slow to prevent hysteresis except very near the transition. Theoretically the response time becomes infinite at the transition.[5] The frequency of the applied field was chosen high enough (1000 Hz) so as to avoid space charge effects; which, from auxillary capacitance bridge measurements, were found to become severe below 100 Hz.

The birefringence fringes were detected by a photodiode and recorded on a strip chart recorder. Voltages were read from a digital voltmeter, which measured the output of an accurate operational amplifier absolute value circuit to the nearest 0.2 millivolt. Recordings were made at intervals of one millivolt in the vicinity of each birefringence maximum and minimum. The voltage corresponding to the ith extremum was determined by interpolating between the two voltages lying nearest to the extremum. In this way V_s could be determined to within one millivolt. The positions of these extrema were found to be reproducible to within one millivolt upon ramping up or down field except near the transition where hysteresis built up to several millivolts. The point at which hysteresis effects became negligible occurred at a reduced voltage (V/V_c) of 1.12. The total number of fringes appearing up to this voltage depends upon cell thickness.

The nematic liquid crystal used in this experiment was a mixture of phenylbenzoate esters whose components are listed in Table I. This mixture has a V_c of approximately 0.7 volt, and a clearing point of 58°C. Data were taken on 100 micron and 50 micron cells over a range of reduced voltages extending to 2.9 and 4.5 respectively. Cell surfaces were prepared by first coating the electrodes with 2000–3000 Å of a polyamide-imide copolymer (Rhodia Kermid 500). Following post cure the polymer surface was rubbed to give homogeneous alignment.

TABLE I

Composition of liquid crystal material used in this study
$X{-}C_6H_4CO_2C_6H_4{-}Y$

Compound	X	Y	Mole fraction
I	n-CH_3O—	n-C_5H_{11}—	0.110
II	n-$C_5H_{11}O$—	n-C_5H_{11}—	0.040
III	n-C_5H_{11}—	CN	0.235
IV	n-C_7H_{15}—	CN	0.322
V	n-$C_5H_{11}O$—	CN	0.182
VI	n-$C_7H_{15}O$—	CN	0.111

BACKGROUND

Two equations appearing in Ref. 2, for a cell with parallel orientation, are relevant to this paper. The first gives the applied voltage as an integral over the molecular orientation in the display.

$$\frac{V'}{V_c} = \frac{2}{\pi}\sqrt{1 + \gamma\eta}\int_0^{\pi/2}\left(\frac{1 + \kappa\eta\sin^2\psi}{(1 + \gamma\eta\sin^2\psi)(1 - \eta\sin^2\psi)}\right)^{1/2} d\psi \tag{5}$$

The second equation gives the optical retardation relative to the zero field.

$$\delta_c = \frac{n_e d}{\lambda}\left[1 - \frac{\displaystyle\int_0^{\pi/2}\left(\frac{(1 + \kappa\eta\sin^2\psi)(1 + \gamma\eta\sin^2\psi)}{(1 + \nu\eta\sin^2\psi)(1 - \eta\sin^2\psi)}\right)^{1/2} d\psi}{\displaystyle\int_0^{\pi/2}\left(\frac{(1 + \kappa\eta\sin^2\psi)(1 + \gamma\eta\sin^2\psi)}{1 - \eta\sin^2\psi}\right)^{1/2} d\psi}\right] \tag{6}$$

The following definitions apply to Eqs. (1) and (2):

$$\eta = \sin^2\phi_m \tag{7}$$

$$\gamma = \frac{\varepsilon_1}{\varepsilon_2} - 1 \tag{8}$$

$$\kappa = \frac{k_{33}}{k_{11}} - 1 \tag{9}$$

$$\nu = \left(\frac{n_e}{n_0}\right)^2 - 1 \tag{10}$$

$$V_c = \pi\left(\frac{k_{11}}{(\varepsilon_1 - \varepsilon_2)\varepsilon_0}\right) \tag{11}$$

$$\sin\psi = \frac{\sin\phi}{\sin\phi_m} \tag{12}$$

Equation (1) is used to determine ϕ_m or η as a function of the applied voltage for a given set of parameters. Once the distribution of $\phi_m(V')$ is determined, the retardation $\delta(V')$ can be calculated from Eq. (2).

CALCULATION PROCEDURE

Splay and bend elastic constants, both components of the dielectric tensor, and cell thickness can be obtained from the experimentally measured retardation, δ_m, using a non-linear curve-fitting algorithm such as Marquardt's Compromise.[6]

Parameter estimates are obtained by minimizing the sum of squares difference between the measured and calculated relative retardation.

$$S = \sum_1^N (\delta_m - \delta_c)_i^2 \tag{13}$$

There are N experimental points and therefore N values of ϕ_m to be determined for a given set of parameters before S can be calculated. A value of ϕ_m corresponding to each V' is obtained by adjusting ϕ_m in Eq. (5) until the difference is less than some pre-selected tolerance, τ.

$$|V' - V_s| \leq \tau \tag{14}$$

For the purpose of this calculation a value of $\tau = 0.0005$ was found to be suitably small. N-values of ϕ_m thus obtained are used in Eq. (6), along with the parameters, to calculate $\delta_c\ (V')$.

The calculations are started by guessing numerical values for each adjustable parameter in the set $\{P\}$. After calculation of S, from Eq. (13), it is necessary to compute the sensitivity of the model to each parameter at each data point.

For the jth parameter at data point i, the sensitivity is approximated numerically.

$$\frac{\partial \delta_{ci}}{\partial P_j} = \frac{\delta_{ci}(P_j + \Delta P_j) - \delta_{ci}(P_j)}{\Delta P_j} \tag{15}$$

Applying Eq. (15) at N-data points for p-parameters generates an $N \times p$ matrix which is used in conjunction with the vector of residuals

$$R_i = (\delta_m - \delta_c)_i \tag{16}$$

to calculate corrections to the latest parameter estimates. Repeated application of this procedure results in a minimum S and a set of statistically determined parameters. Parameter covariance, confidence limits, and t-values are readily determined from the calculations. Details of the statistical analysis and development of the algorithm are given in Refs. 6–9.

Integration of Eqs. (5) and (6) was performed using ten-point gaussian quadrature, although a multi-step numerical integration should be more accurate.

COMPUTATIONAL RESULTS

Equations (5) and (6) contain seven parameters, excluding λ, which, in principle, can be adjusted to minimize S. The complete parameter set is $\{k_{11}, k_{33}, \varepsilon_1, \varepsilon_2, n_e, n_0, d\}$ which can be transformed by lumping parameters to obtain $\{V_c, \kappa, \gamma, v, d, n_e\}$. The wavelength is treated as an experimentally fixed constant as its value is known to five significant figures.

It is often difficult to obtain proper convergence and minimum S when attempting to adjust a large number of parameters. Convergence depends on the shape of the sum of squares surface which may contain relative minima in parameter space. The first problem is then to select a suitable subset of parameters, from the set of seven above, which will converge to give a true minimum S.

The initial choice for an adjustable set consisted of only three parameters $\{V_c, \kappa, \gamma\}$ with $\{\varepsilon_1, \varepsilon_2, n_e, n_0, d\}$ being measured independently. Elastic constants are obtained from V_c and κ using Eqs. (9) and (11). γ can be calculated using experimental values of ε_1 and ε_2 in Eq. (8) and the result compared to the parameter estimate.

There are two shortcomings associated with the three parameter set $\{V_c, \kappa, \gamma\}$ which eliminate it from contention as the final choice for an adjustable set. First, the parameters V_c, κ, and γ are coupled in that V_c contains elements of κ and γ. Coupling is undesirable in that large parameter covariance is built into the model. As a consequence, it is often difficult to obtain accurate parameter estimates with narrow confidence limits for a coupled set. The second reason is simply that using only three of seven potentially estimatable parameters does not represent efficient use of the data set and model.

A second attempt to obtain convergence to minimum S was made using all seven parameters. The results are shown in Table II. The reduction in σ realized by going from three to seven parameters is a result of uncoupling, and by obtaining a better estimate of cell thickness than independent measurements provided. Since the standard deviation for seven parameters was so much less than obtained using three, it was thought all seven could be determined using the least squares algorithm. Further numerical testing of the model revealed a serious flaw in that different initial guesses of the parameters produced different final values for n_e, n_0, and d even though σ remained in the 10^{-6} range.

TABLE II

Standard deviation for various parameter sets
(105 μm cell)

Adjustable parameters	Standard deviation
3 $\{V_c, \kappa, \gamma\}$	8.5×10^{-5}
5 $\{k_{11}, k_{33}, \varepsilon_1, \varepsilon_2, d\}$	1.37×10^{-6}
7 $\{k_{11}, k_{33}, \varepsilon_1, \varepsilon_2, d, n_e, n_0\}$	1.23×10^{-6}

Examination of the data in Table III shows the problem more clearly. The first four parameters, k's and ε's, have narrow confidence limits and large t-values. However, very little confidence can be associated with n_e, n_0, and d as reflected in their wide confidence regions and low t-values. In fact, these

TABLE III

Estimates, confidence limits, and values for seven adjustable parameters

Parameter and estimate		95% confidence limits	t-value
$k_{11} \times 10^7$	6.11	6.08 – 6.15	3403
$k_{33} \times 10^7$	11.96	11.88 – 12.04	3139
ε_1	20.76	20.61 – 20.91	2841
ε_2	6.27	6.24 – 6.31	2708
n_e	1.6816	1.5193– 1.8439	216
n_0	1.5054	1.3755– 1.6353	241
$d \times 10^4$	105.28	85.73 –124.83	112

last three parameters were observed to vary over a broad range and settle upon final values which were physically unacceptable on many occasions.

The quantity $(n_e - n_0)d/\lambda$ is the important term with respect to fringing, however. The net effect is high covariance between n_e, n_0, and d indicating these parameters are strongly coupled.

Since covariance between n_e, n_0, d and the k's and ε's is low, it is possible to select one parameter from the former subset for inclusion into the latter. The optimum set for this problem then becomes one containing five parameters and appears in Table II. n_e and n_0 can be measured independently using an Abbe' refractometer as previously mentioned.

Data in Table IV illustrates the sensitivity of the parameters to errors in n_e and n_0, and also shows the effects of covariance between n_e, n_0, and d. An arbitrary error of ±0.005 was selected with translates into a 0.3 percent error in n_e and n_0. The corresponding range in d is 2.7 percent which is an order of magnitude greater. The product $d\,(n_e - n_0)$ remains constant however, which means that changes in n_e or n_0 are compensated for by changes in d, In this illustration n_e and n_0 were changed very little, but in actual practice,

TABLE IV

Parameter sensitivity to errors in n_e and n_0

		$\times 10^7$					
Index	$\sigma \times 10^6$	k_{11}	k_{33}	ε_1	ε_2	$d \times 10^4$	$d(n_e + n_0)$
$n_0 + 0.005$	1.42	6.19	11.69	20.94	6.35	107.79	18.45
$n_0 = 1.5054$	1.37	6.16	11.81	20.88	6.38	104.92	18.49
$n_0 = 0.005$	1.53	6.18	1185	20.93	6.39	101.96	18.48
$n_e + 0.005$	1.42	6.20	11.81	20.96	6.57	101.85	18.46
$n_e = 1.6816$	1.37	6.16	11.81	20.88	6.38	104.92	18.49
$n_e - 0.005$	1.32	6.21	11.75	21.00	6.35	107.80	18.46

with seven adjustable parameters, large variations in n_e and n_0 were also compensated for by changes in d. Thus covariance between these three parameters is seen to be large. The small improvement in σ realized by decreasing n_e may be indicative of some experimental error in its initial determination, although covariance obscures the truth.

The other four parameters are seen to be relatively unaffected by small changes in n_e and n_0.

EXPERIMENTAL RESULTS

Cell thickness was found to have the greatest influence on parameter estimates in that determinations using the 50 μm cell were significantly different from those based on the 105 μm cell. The comparisons are shown in Table V.

TABLE V

A comparison of results obtained from 105 and 50 μm thick cells

Standard Deviation	1.37×10^{-6}	1.24×10^{-6}
k_{11} (dynes)	6.16×10^{-7}	6.18×10^{-7}
k_{33}	11.81×10^{-7}	13.47×10^{-7}
ε_1	20.88	19.96
ε_2	6.38	6.39
d (microns)	104.92	49.75
V_c	0.688	0.718
ε_a	14.50	13.57
γ	2.27	2.12
κ	0.92	1.18
N	37	24
	95% Confidence Limits	
k_{11}	6 12– 6.18	6.11–6.25
k_{33}	11.75–11.86	13.30–13.63
ε_1	20.82–20.94	19.84–20.08
ε_2	6.33–6.42	6.28–6.51
d	104.77–105.07	49.62–49.88

The salient features of this comparison are contained in the confidence limits. Confidence intervals for k_{33} and ε_1 determined for the thick and thin cells do not overlap. The confidence intervals of k_{11} and ε_2 for the thin cell completely envelop their respective intervals of the thick cell. As a consequence k_{11} and ε_2 are accurately determined, but cell thickness appears to influence the other two parameter estimates. Additional experimental work will determine whether this is truly a cell thickness effect or an effect due to surface preparation or some other experimental parameter not presently recognized as important.

Leaving aside the problem of cell thickness for the moment, the readers' attention is directed to Table VI. Almost all of the difference between Dueling's theory and experiment shows up at low V/V_c. No variance was found when $V/V_c \geq 1.15$ although this ratio was slightly lower for the thin cell.

TABLE VI

Parameter variation as influenced by hysteresis at low (V/V_c)

N	$\sigma \times 10^6$	V/V_c[a] Min	V/V_c[a] Max	ϕ_m Min	ϕ_m Max	d[b]	k_{11}	k_{33}	ε_1	ε_2	Fringes Removed
44	3.83	1.012	2.95	6.3	80.1	105.11	6.17	11.85	20.95	6.49	NONE
43	2.96	1.008	2.95	5.0	80.1	105.63	5.98	11.77	20.65	6.75	#10—a bad data point
42	2.63	1.038	2.95	11.3	80.1	105.23	6.05	11.72	20.70	6.55	0, 10
41	1.92	1.064	2.95	14.3	80.1	104.89	6.17	11.78	20.85	6.31	0, 1, 10
40	1.72	1.086	2.95	16.8	80.1	104.82	6.21	11.85	21.00	6.35	0, 1, 2, 10
37	1.37	1.17	2.95	24.1	80.1	104.92	6.16	11.81	20.88	6.38	0–5, 10
36	1.47	1.196	2.95	25.8	80.1	105.04	6.14	11.87	20.85	6.34	0–6, 10
25	20.3	0.98	4.54	—	87.7	50.23	6.63	15.41	22.74	8.39	NONE
24	1.24	1.06	4.54	14.0	87.7	49.75	6.18	13.47	19.96	6.39	0
23	1.31	1.13	4.54	20.1	87.7	49.65	6.16	13.25	19.67	6.09	0, 1
21	1.32	1.23	4.54	28.4	87.7	49.98	5.87	12.79	19.45	6.90	0–3
17	1.38	1.47	4.54	41.2	87.7	49.87	5.94	12.86	19.33	6.51	0–7

[a] The largest and smallest V/V_c for N points are shown

[b] d is in microns; k_{11} and $k_{33} \times 10^7$

Forty-four points constitute the complete data set for the thick cell starting with the zeroth fringe. After removal of fringe ten which was a bad data point, σ decreased to 2.96×10^{-6}. Removing six additional fringes at low voltage produces a reduction in σ to 1.37×10^{-6} at a V/V_c minimum of 1.17. Removing one more fringe resulted in an increase in σ which indicates the degrees of freedom $(N - p)$ are going down faster than error is being reduced resulting in a loss of significance. Improvement in σ is more striking for the thin cell as removal of only one point, the zeroth fringe, caused σ to decrease from 20.3×10^{-6} to 1.24×10^{-6}. Distortion of the fringing pattern at low V/V_c can be explained on the basis that response time scales to infinity as the applied field approaches the critical field.[5] The magnitude of the distortion is then related to how rapidly one wishes to conduct an experiment of this type.

At the maximum, $V/V_c = 4.5$, $\phi_m = 87.7$ degrees, and no significant difference between theory and experiment could be detected. This is important from the point of view of Frank's theory being a small distortion theory, and differences would be expected at high V/V_c.

An attempt to account for the thickness discrepancy in k_{33} and ε_1 was made by testing the theory using small non-zero angles for molecules adjacent to the surfaces. Angles in the range $0 \leq \phi(z = 0) \leq 5$ degrees were examined, and the data appears in Table VII. No convincing evidence was found relating to the discrepancy, although it is possible to match ε_1 by allowing the 50 μm cell to have a zero surface angle and the 105 μm cell a five degree angle. For this condition to exist, however, σ should be a minimum at five degrees for the 105 μm cell. This is not the case as can be seen in Table VII; therefore a non-zero surface angle can be ruled out. The occurrence of minimum σ at zero degrees also implies identical surface treatments on both test cells insofar as these data are concerned. Similar arguments apply to k_{33}.

TABLE VII

Surface angle effects on parameter estimates

		$\times 10^7$				
Angle	$\sigma \times 10^6$	k_{11}	k_{33}	ε_1	ε_2	d
0	1.37	6.16	11.81	20.88	6.38	104.92
1	1.60	6.21	11.97	20.52	6.29	105.1
2	1.75	6.24	12.02	20.21	6.36	105.2
3	1.75	6.49	12.55	20.39	6.29	105.2
4	1.93	6.53	12.61	20.01	6.24	105.3
5	2.55	6.39	12.58	19.44	6.45	105.7
0	1.24	6.18	13.47	19.96	6.39	49.75
1	1.28	6.31	13.65	19.69	6.13	49.69
2	1.33	6.30	13.82	19.30	6.08	49.76
3	1.35	6.28	13.65	18.69	5.89	49.73
4	1.63	6.65	14.25	19.16	6.20	49.76
5	1.79	6.45	14.27	18.54	6.09	49.84

CONCLUSIONS

Deuling's theory is satisfactory for nematics of high positive anisotropy over a wide range of V/V_c values.

Discrepancies between theory and experiment at low V/V_c are not important sources of error in view of the inherent slowing of cell response near V_c.

All parameters can be estimated with narrow confidence limits. Both k_{11} and ε_2 can be estimated accurately using the experimental method described herein. k_{33} and ε_1 are obviously thickness dependent with differences between cells being 21 and 5 percent, respectively.

Small non-zero surface angles apparently do not play a significant role in the thickness dependence problem.

Accurate estimation of k_{33} and ε_1 should be possible using thick cells, although final determination of this can only be made by studying the thickness dependence of these two parameters.

Acknowledgements

The authors would like to thank Dr. Alfred Saupe for directing our attention to Deuling's paper, and for taking time to discuss the results of this paper.

GLOSSARY

d	cell thickness
I	transmitted light intensity Eq. (1)
k_{ii}	Frank elastic constants ($i = 1$, splay; $i = 3$, bend)
n_e	extraordinary index of refraction
n_0	ordinary index of refraction
N	number of data points
p	number of adjustable parameters
R	vector of residuals Eq. (16)
S	sum of squares Eq. (13)
V_c	critical voltage defined by Eq. (11)
V_s	applied test voltage
V'	calculated voltage Eq. (5)
γ	parameter defined by Eq. (8)
δ_c	calculated relative retardation Eq. (6)
δ_m	measured relative retardation
ε_1	parallel component of the dielectric tensor
ε_2	perpendicular component of the dielectric tensor
κ	parameter defined by Eq. (9)
λ	wavelength of light used for experimental purposes -6328 Å
η	constant of the voltage defined by Eq. (7)
ν	parameter defined by Eq. (10)
σ	standard deviation
ϕ_m	angle of the director at $d/2$
ψ	angle defined by Eq. (12)

References

1. F. C. Frank, *Disc. Faraday Soc.*, **25**, 19 (1958).
2. H. J. Deuling, *Mol. Cryst. Liq. Cryst.*, **19**, 123 (1972).
3. H. Gruler and G. Meier, *Mol. Cryst. Liq. Cryst.*, **16**, 299 (1972).
4. A. Saupe, *Z. Naturforschg*, **15a**, 818 (1960).
5. F. Brochard, *Mol. Cryst. Liq. Cryst.*, **23**, 51 (1973).
6. D. W. Marquardt, *J. Soc. Indust. Appl. Math.*, **11** (2), 431 (1963).
7. C. Maze and G. Burnet, *Surface Sci.*, **13**, 451 (1970).
8. H. O. Hartley, *Technometrics*, **3** (2), 269 (1961).
9. C. Daniel and F. Wood, Fitting equations to data, computer analysis of multifactor data for scientists and engineers. (Wiley, New York, 1971).